Rigorous close-coupling quantum dynamics calculation of thermal rate constants for the water formation reaction of H_2 + OH on a high-level PES

Ralph Welsch

Citation: The Journal of Chemical Physics **148**, 204304 (2018); doi: 10.1063/1.5033358
View online: https://doi.org/10.1063/1.5033358
View Table of Contents: http://aip.scitation.org/toc/jcp/148/20
Published by the American Institute of Physics

Rigorous close-coupling quantum dynamics calculation of thermal rate constants for the water formation reaction of H_2 + OH on a high-level PES

Ralph Welsch[a)]
Center for Free-Electron Laser Science, DESY, Notkestrasse 85, 22607 Hamburg, Germany

(Received 5 April 2018; accepted 27 April 2018; published online 29 May 2018)

Thermal rate constants for the prototypical H_2 + OH → H + H_2O reaction are calculated using quantum dynamics simulations including all degrees of freedom and accurately accounting for overall rotation via close-coupling. Results are reported for a recent, highly accurate neural network potential [J. Chen *et al.*, J. Chem. Phys. **138**, 154301 (2013)] and compared to results obtained on a previous, semi-empirical potential. Thermal rate constants between 300 K and 1000 K are reported and very good agreement with experimental work is found. Additionally, reasonable agreement for the close-coupling simulations on both potentials is found. In contrast to previous work, we find that the J-shifting approximation works well for the title reaction given that a high-level PES is used for the dynamics calculation. Moreover, the importance of treating the spin-orbit coupling in the reactant partition function is discussed. The highly accurate results reported here will provide a benchmark for the development of approximate methods. *Published by AIP Publishing.* https://doi.org/10.1063/1.5033358

I. INTRODUCTION

The reaction of H_2 + OH is one of the main routes for water formation in the interstellar medium[1–4] and is an important prototypical reaction for combustion and atmospheric chemistry.[5–7] Thus, its reaction dynamics and kinetics have attracted considerable theoretical and experimental work.[6,8–12] However, to date, the only full-dimensional quantum dynamical calculation of thermal reaction rate constants for the title reaction that accurately accounts for overall rotation has been performed on an inaccurate semi-empirical potential energy surface (PES) developed in 1980.[13,14]

The last two decades have brought about major advances in the creation of highly accurate PES for polyatomic systems[15–17] based on routinely available high level, i.e., coupled-cluster singles doubles and perturbative triples (CCSD(T)), *ab initio* calculations. For the title reaction, Zhang and co-workers presented a globally accurate Shepard interpolated PES based on CCSD(T) energies in 2001 (YZCL2)[18] and an improved version in 2011 (XXZ).[9] Bowman and co-workers presented an accurate global PES employing permutationally invariant polynomials (FKB).[19] A very accurate and computationally efficient global PES based on neural networks (NN) was developed recently (NN1).[20] Despite these advances, no rigorous quantum dynamical calculation of thermal rate constants including overall rotational motion and employing accurate *ab initio* potentials has been performed for any poly-atomic system. Additionally, full-dimensional quantum dynamics calculations of rate constants employing the J-shifting approximation are only available for a few polyatomic reactions.[21–27]

Most accurate thermal rate constant calculations for polyatomic molecules employ the quantum transition state concept[28–35] and the multi-configurational time-dependent Hartree (MCTDH) approach.[36,37] The quantum transition state concept has been proven as the most efficient method to treat the reaction dynamics of polyatomic systems rigorously.[22,35,38–47] The quantum transition state concept is particularly efficient for the calculation of thermal rate constants. In the quantum transition state concept, the eigenstates of the thermal flux operator, which represent the relevant vibrational states of the activated complex, are employed. These eigenstates, which are located in the transition state region, are then propagated toward the reactant and product asymptotic area. To obtain thermal rate constants, only short time propagation is required. The wave-packet propagation for polyatomic systems can be efficiently carried out using the MCTDH approach[36,37] and its various extensions.[33,48–52]

Besides the exact calculation of thermal rate constants employing the quantum transition state concept, various approximate methods have been employed to calculate thermal rate constants on modern PES. Successful approximate approaches include instanton calculations,[53] the ring-polymer molecular dynamics (RPMD) approach,[54,55] and various semi-empirical tunneling corrections to transition state theory (TST).[56] All these approaches have been employed to study the title reaction.[57,58] It should also be noted that, while RPMD and semi-empirically corrected TST account for overall rotation, this is not true for instanton calculations, which employ the J-shifting approximation,[59] which previously has been assessed to give significant errors for the title reaction.[13]

In this article, accurate full-dimensional close-coupling calculations of the thermal rate constant for the title reaction are presented. The article is organized as follows. In Sec. II, the

[a)]Electronic mail: ralph.welsch@desy.de

underlying theory and computational methods are described. Section III presents the system details and parameters. The results are presented and discussed in Sec. IV, and the main conclusions are presented in Sec. V.

II. METHODS

A. Quantum transition state concept

The quantum transition state concept provides an established framework for the calculation of thermal rate constants.[23,28–35,60–70] This work employs the scheme introduced in Ref. 32 and slightly revised in Ref. 33.

The quantum transition state concept is based on flux-flux correlation functions. The cumulative reaction probability (CRP) is given as

$$N(E) = 2\pi^2 \, \mathbf{tr}\Big(\widehat{F}\,\delta(E-\widehat{H})\widehat{F}\,\delta(E-\widehat{H})\Big), \tag{1}$$

where $\hat{F} = -i[\hat{H}, h]$ denotes the flux operator and h is a Heaviside step function that equals 1 on the product side and 0 on the reactant side of the dividing surface of the reaction. Within the present scheme, the thermal flux operator,[71]

$$\widehat{F}_{T_0} = \mathrm{e}^{-\frac{\widehat{H}}{2kT_0}}\widehat{F}\mathrm{e}^{-\frac{\widehat{H}}{2kT_0}} = \sum_{f_{T_0}} |f_{T_0}\rangle f_{T_0}\langle f_{T_0}|, \tag{2}$$

at a reference temperature T_0, is employed to evaluate the trace. Thus the CRP can be written as

$$N(E) = \frac{1}{2}\,\mathrm{e}^{\frac{E}{kT_0}} \int \mathrm{d}t \int \mathrm{d}t' \, \mathrm{e}^{iEt}\,\mathrm{e}^{-iEt'} \sum_{f_{T_0}} f_{T_0}\Big\langle f_{T_0}\Big|\mathrm{e}^{i\widehat{H}t'}\widehat{F}\mathrm{e}^{-i\widehat{H}t}\Big|f_{T_0}\Big\rangle \tag{3}$$

or as

$$N(E) = \frac{1}{2}\,\mathrm{e}^{\frac{E}{kT_0/2}} \sum_{f_{T_0}}\sum_{f'_{T_0}} f_{T_0}f'_{T_0}\left|\int \mathrm{d}t\, \mathrm{e}^{iEt}\Big\langle f_{T_0}\Big|\mathrm{e}^{-i\widehat{H}t}\Big|f'_{T_0}\Big\rangle\right|^2. \tag{4}$$

Thermal rate constants are obtained from $N(E)$,

$$k(T) = \frac{1}{2\pi Q_r(T)} \int \mathrm{d}E\, N(E)\,\mathrm{e}^{-\frac{E}{kT}}. \tag{5}$$

Here $Q_r(T)$ denotes the partition function of the reactants. In the present work, the partition function is calculated as

$$Q_r(T) = \frac{1}{\sigma}\, Q_{\mathrm{rot}}(T)\, Q_{\mathrm{vib}}(T)\, Q_{\mathrm{trans}}(T)\, Q_{\mathrm{elec}}(T), \tag{6}$$

$$Q_{\mathrm{rot}}(T) = (kT \cdot 2\, I_{\mathrm{H_2}}) \cdot (kT \cdot 2\, I_{\mathrm{OH}}), \tag{7}$$

$$Q_{\mathrm{vib}}(T) = \prod_{i=1}^{2} \frac{\mathrm{e}^{-0.5\hbar\omega_i/kT}}{1-\mathrm{e}^{-\hbar\omega_i/kT}}, \tag{8}$$

$$Q_{\mathrm{trans}}(T) = \left(\sqrt{\frac{mkT}{2\pi\hbar}}\right)^3, \tag{9}$$

with σ being the symmetry factor, $I_{\mathrm{H_2}}$ and I_{OH} being the moments of inertia of H_2 and OH, respectively, ω_1 and ω_2 being the harmonic frequencies of H_2 and OH, respectively, and m being the reduced mass of the scattering coordinate. The electronic partition function $Q_{\mathrm{elec}}(T)$ contains a factor due to spin-orbit splitting of magnitude ΔE, which is neglected in the construction of the PES and therefore also in the dynamics. It can be approximated in two ways,[72]

$$Q_{\mathrm{elec}}(T) = \left(1 + \mathrm{e}^{-\Delta E_{\mathrm{elec}}/kT}\right) \tag{10}$$

or

$$Q_{\mathrm{elec}}(T) = \left(\mathrm{e}^{\Delta E_{\mathrm{elec}}/2kT} + \mathrm{e}^{-\Delta E_{\mathrm{elec}}/2kT}\right). \tag{11}$$

The first approach assumes that the given spin-orbit free state is the correct ground state and assumes that the spin-orbit excited state is ΔE higher. The second approach assumes that the given spin-orbit free state is an equal average of both spin-orbit split states and thus that the true ground state is $\Delta E/2$ lower and the spin-orbit excited state is $\Delta E/2$ higher than the given state. The latter approach performs better for the $Cl + H_2 \rightarrow HCl + H$ reaction, where potentials with spin-orbit coupling and without spin orbit coupling are available.[72] As both the Schatz-Elgersma (SE) and NN1 PESs are constructed from electronic structure data that do not include spin-orbit splitting, the latter approach is the logical consistent way to account for spin-orbit splitting in this work. Alternatively, the spin-orbit coupling can be neglected, and a factor of two is added to the partition function as only one of the initial electronic states is reactive.

In previous work, it was found that splitting the imaginary time propagation can increase the numerical stability.[13,23–25,73] This scheme is also employed in the present work, and consequently, Eq. (4) is replaced by

$$N(E) = \frac{1}{2}\,\mathrm{e}^{\frac{2E}{kT_2}} \sum_{f_{T_1}}\sum_{f'_{T_1}} f_{T_1}f'_{T_1} \times \left|\int \mathrm{d}t\, \mathrm{e}^{iEt}\Big\langle f_{T_1}\Big|\mathrm{e}^{-\widehat{H}\beta_2}\,\mathrm{e}^{-i\widehat{H}t}\,\mathrm{e}^{-\widehat{H}\beta_2}\Big|f'_{T_1}\Big\rangle\right|^2, \tag{12}$$

where $T_1 > T_2$ is a higher reference temperature used to initially calculate the thermal flux eigenstates. After that, these eigenstates are propagated in imaginary time for $\beta_2 = \frac{1}{2}(\frac{1}{kT_2} - \frac{1}{kT_1})$. A similar modification can also be used for Eq. (3).

Furthermore, a harmonic extrapolation is used to account for the non-explicitly treated thermal flux eigenstates. If the $N(E)$ calculation includes n thermal flux eigenstate pairs, the best estimate for the rate constant reads[74]

$$k(T) = \frac{1}{2\pi Q_r(T)} \frac{\sum_{i=0}^{\infty}\exp(-(E_i-E_0)/k_BT)}{\sum_{i=0}^{n-1}\exp(-(E_i-E_0)/k_BT)} \int \mathrm{d}E\, N(E)\,\mathrm{e}^{-\frac{E}{kT}}, \tag{13}$$

where E_i is the energy of the ith vibrational state of the activated complex in the harmonic approximation.

Overall rotational motion can be considered using a statistical sampling approach.[60,69,75,76] In this approach, a set of M random rotational wave functions $|\Psi^{(j)}_{\mathrm{rot}}\rangle$ ($j = 1, \ldots, M$) is used to define a statistical thermal flux operator,

$$\widehat{F}^j_{T_0} = \mathrm{e}^{-\frac{\widehat{H}}{2kT_0}}\widehat{F}|\Psi^{(j)}_{\mathrm{rot}}\rangle\langle\Psi^{(j)}_{\mathrm{rot}}|\mathrm{e}^{-\frac{\widehat{H}}{2kT_0}}, \tag{14}$$

where the rotational wave functions are defined as

$$|\Psi^{(j)}_{\mathrm{rot}}\rangle = \sum_{J=0}^{J_{\max}} \sum_{K=-\mathrm{Min}(J,K_{\max})}^{\mathrm{Min}(J,K_{\max})} (-1)^{\alpha_{J,K}(j)}\sqrt{2J+1}|JKM\rangle \tag{15}$$

with $\alpha_{J,K}(j)$ being the random integer numbers, $|JMK\rangle$ being the Wigner rotation matrices, and the quantum number M chosen arbitrarily. The projector $|\Psi_{\rm rot}^{(j)}\rangle\langle\Psi_{\rm rot}^{(j)}|$ commutes with the flux operator $\widehat{F}$, and the random functions fulfill the completeness relation,

$$1 = \lim_{M\to\infty} \frac{1}{M} \sum_{j=1}^{M} |\Psi_{\rm rot}^{(j)}\rangle\langle\Psi_{\rm rot}^{(j)}|. \tag{16}$$

Therefore, the standard flux operator can be written as

$$\widehat{F}_T = \lim_{M\to\infty} \frac{1}{M} \sum_{j=1}^{M} \widehat{F}_T^j. \tag{17}$$

While the eigenstates of the thermal flux operator correspond to rovibrational states of the activated complex, the eigenstates of the statistical thermal flux operator $\widehat{F}_T^j$ correspond to vibrational states. Due to the projection $|\Psi_{\rm rot}^{(j)}\rangle\langle\Psi_{\rm rot}^{(j)}|$, the rotational progression disappears from the spectrum of the statistical thermal flux operator. Thus, the eigenstates of $\widehat{F}_T^j$ can efficiently be computed by an iterative diagonalization approach. The CRP is obtained analogously to Eq. (3) as

$$N(E) = \lim_{M\to\infty} \sum_{j=1}^{M} \frac{1}{2}\, \mathrm{e}^{\frac{E}{kT_0}} \int \mathrm{d}t \int \mathrm{d}t'\, \mathrm{e}^{iEt}\, \mathrm{e}^{-iEt'} \times \sum_{f_{T_0}^{(j)}} f_{T_0}^{(j)} \left\langle f_{T_0}^{(j)} \middle| \mathrm{e}^{i\widehat{H}t'} \widehat{F} \mathrm{e}^{-i\widehat{H}t} \middle| f_{T_0}^{(j)} \right\rangle. \tag{18}$$

If rotational and internal motion can be considered to be separable, only the internal motion has to be taken into account in the dynamics simulations. The full thermal rate constant can be approximated employing the J-shifting scheme[59] as

$$k(T) = \frac{Q_{rot}^{\ddagger}(T)}{2\pi Q_r(T)} \int \mathrm{d}E\, N_{J=0}(E)\, \mathrm{e}^{-\frac{E}{kT}}, \tag{19}$$

where $Q_{rot}^{\ddagger}$ is the (classical) rotational partition function at the transition state given as

$$Q_{rot}^{\ddagger}(T) = \sqrt{\pi (2kT)^3 I_1^{\ddagger} I_2^{\ddagger} I_3^{\ddagger}}, \tag{20}$$

where the moments of inertia at the transition state, $I_1^{\ddagger}$, $I_2^{\ddagger}$, and $I_3^{\ddagger}$, are given in Table I.

TABLE I. Parameters employed in the calculation of the partition functions.

Parameter	SE PES	NN1 PES
σ	2	2
I_{H_2} (a.u.)	1 800.0	1 806.32
I_{OH} (a.u.)	5 861.0	5 813.73
I_1 (a.u.)	4 078.66	5 948.79
I_2 (a.u.)	37 519.9	38 242.44
I_3 (a.u.)	41 598.5	44 191.22
ω_1 (cm^{-1})	4 192	4 398
ω_2 (cm^{-1})	3 573	3 741
m (a.u.)	3 309	3 309
$\Delta E_{\rm elec}$ (cm^{-1})	140	140

B. Quantum dynamics

The calculation of the thermal flux eigenstates as well as the subsequent imaginary and real time propagation requires an efficient scheme for high-dimensional wave-packet propagation. Thus, the multi-configurational time-dependent Hartree[36,37] (MCTDH) approach is employed.

The ansatz for a set of MCTDH wave functions within the state-averaged approach[33] reads

$$\Psi_w(x_1,\ldots,x_d,t) = \sum_{j_1=1}^{n_1} \cdots \sum_{j_d=1}^{n_d} A^1_{w;j_1\ldots j_d}(t) \prod_{k=1}^{d} \Phi^{1;k}_{j_k}(x_k,t). \tag{21}$$

In this two-layer representation, time-dependent basis functions $\Phi^{1;k}_{j_k}(x_k,t)$, called single-particle functions (SPFs), are used. They are subsequently expanded in a time-independent basis $\{\chi^k_j(x_k)\}$,

$$\Phi^{1;k}_{j_k}(x_k,t) = \sum_{i_k=1}^{N_k} A^{2;k}_{j_k;i_k}(t)\chi^k_{i_k}(x_k). \tag{22}$$

This approach can be extended to a multi-layer (ML) representation,[48,49] where the SPFs are recursively expanded in a time-dependent basis. Considering, e.g., two layers of SPFs, the multi-layer (ML) MCTDH ansatz reads

$$\begin{aligned}
\Psi_w\left(x^1_1,\ldots,x^1_d,t\right) &= \sum_{j_1=1}^{n_1} \cdots \sum_{j_d=1}^{n_d} A^1_{w;j_1\ldots j_d}(t) \prod_{k=1}^{d} \Phi^{1;k}_{j_k}\left(x^1_k,t\right),\\
\Phi^{1;k}_p\left(x^1_k,t\right) &= \Phi^{1;k}_p\left(x^{2;k}_1,\ldots,x^{2;k}_{d_k},t\right)\\
&= \sum_{j_1=1}^{n_{k,1}} \cdots \sum_{j_p=1}^{n_{k,d_k}} A^{2;k}_{p;j_1\ldots j_{d_k}}(t) \prod_{l=1}^{d_k} \Phi^{2;k,l}_{j_l}\left(x^{2;k}_l,t\right),\\
\Phi^{2;k,\lambda}_p\left(x^{2;k}_\lambda,t\right) &= \sum_{j=1}^{N_\alpha} A^{3;k;\lambda}_{p;j}(t)\chi^\alpha_j\left(x^{2;k}_\lambda\right),
\end{aligned}$$

with

$$\alpha = \lambda - \sum_{i=1}^{k-1} d_i.$$

An efficient scheme for the propagation of MCTDH wave functions is the constant mean-field (CMF) integration.[77] This work uses a revised version, the CMF2 scheme.[78] Matrix elements of a general potential energy surface (PES) are obtained using the correlation discrete variable representation (CDVR)[50] scheme with its multi-layer extension (ML-CDVR)[49,51] throughout this work.

III. SYSTEM DETAILS

Hyperspherical coordinates employing reactant Jacobi coordinates are used in this work. r_1, r_2, and R denote the H–H, O–H, and H–H center of mass to O–H center of mass distances, respectively. θ_1 and θ_2 are the angles between $\vec{r}_1$ and $\vec{R}$ and between $\vec{r}_2$ and $\vec{R}$, respectively. The angle φ describes the torsional motion. The hyperspherical coordinates ρ and α are obtained from r_1 and R as

$$\rho = \sqrt{\mu_R R^2 + \mu_1 r_1^2}, \tag{23}$$

$$\alpha = \arctan\left(\frac{\sqrt{\mu_R}R}{\sqrt{\mu_1}r_1}\right), \tag{24}$$

with the reduced masses

$$\mu_1 = \frac{m_H}{2}, \tag{25}$$

$$\mu_2 = \frac{m_H m_O}{m_H + m_O}, \tag{26}$$

$$\mu_R = \frac{(m_H + m_H)(m_H + m_O)}{m_H + m_H + m_H + m_O}, \tag{27}$$

where m_H is the proton mass and m_O is the oxygen mass. A body fixed frame is defined with the R-axis being the z-axis of the frame and the r_2-axis lying in the x-z-plane of the body fixed coordinate system. The kinetic energy operator in these coordinates is given in Ref. 13. The hyperspherical angle α is employed as a reaction coordinate, and the corresponding flux operator reads

$$\widehat{F} = \frac{i}{\rho^2}\left[\frac{\partial^2}{\partial\alpha^2}, \theta(\alpha - \alpha_0)\right], \tag{28}$$

where $\theta(x)$ is the Heaviside function and $\alpha_0 = 1.30$ a.u. locates the dividing surface close to the transition state.

Both the Schatz-Elgersma (SE) PES[14] and the neural network-based PES (NN1) developed by Zhang and coworkers[20] are employed in this work. In the statistical treatment of the rotational motion, five samples, i.e., $M = 5$, have been sufficient to obtain rate constants for most basis sets employed with a statistical error of less than 10%. A propagation time of 25 fs (SE PES) or 30 fs (NN1 PES) was used. 15 pairs of thermal flux eigenstates have been employed at a reference temperature of $T_1 = 2000$ K. These eigenstates have then been thermalized down by imaginary time propagation to a temperature of $T_2 = 1200$ and $T_2 = 800$ K before the real time propagation has been performed. Employing the formula given in Eq. (4), CRP at half the employed temperature, i.e., at 1000 K, 600 K, and 400 K, can be obtained for the rate constants employing J-shifting. Details of the employed basis sets as well as convergence studies are given in the supplementary material. The particular values of the constants employed in the partition function calculations [Eq. (6)] of this work are given in Table I.

IV. RESULTS

A. Close-coupling calculations

Accurate thermal rate constants on the NN1 PES in the temperature range from 300 K to 1000 K are presented in Fig. 1 and Table II. Based on convergence studies presented in the supplementary material, the error in the new results is estimated to be less than 10% for the temperature range between 300 K and 600 K. At the highest temperature employed, effects due to the limited number of thermal flux eigenstates that can be employed are resulting in a slightly larger error. It should also be noted that all results presented in the main text employ a low reference temperature to obtain reliable results in the low to mid temperature range. To obtain more reliable results at high temperatures, results obtained with a higher reference temperature, as presented in the supplementary material, should be used. Additionally, rates calculated on the semi-empirical SE PES with a much larger basis set as compared

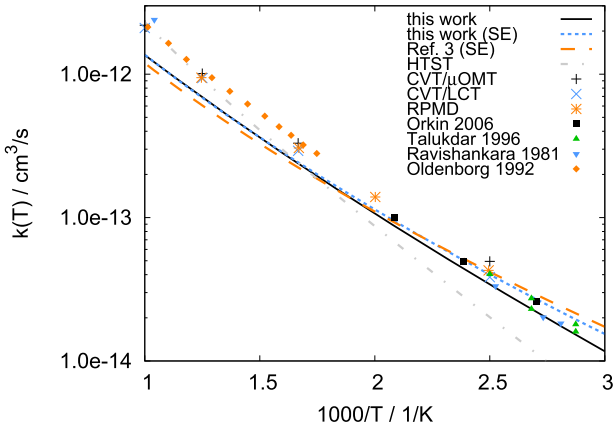

FIG. 1. Thermal rate constants k(T) in cm^3/s for the title reaction. Rigorous close-coupling results on the NN1 and SE PESs are given as a black line and a blue dotted line, respectively. For comparison, various other theoretical and experimental results are given: Previous close-coupling results[13] on the SE PES are given as an orange dashed line. Harmonic TST (HTST) results[57] are given as a gray dashed-dotted line. Semi-empirically corrected TST results[57] are given as black pluses and blue crosses. Results obtained from RPMD[58] are given as orange stars. Theoretical results employ the NN1 PES if not stated otherwise. Filled symbols give experimental results.[79–82]

to previous work[13,32] are presented in Fig. 1 and Table II. The rates calculated for the SE PES are in very good agreement with previous work.[13] Comparing the accurate close-coupling results on both surfaces, a difference of up to 50% is observed. Most noticeably is the difference toward the lower temperature and the slightly different shape of k(T). The accurate thermal rate constants on the NN1 PES agree well with experimental results[79–82] and are within the experimental error bars. At the highest temperatures employed, larger deviations are found due to the higher errors of the close-coupling results at higher temperatures, as discussed above. Good agreement is also found with the approximate rates obtained by RPMD[58] and semi-empirically corrected TST, while less good agreement is found for results obtained by harmonic TST (HTST).

B. J-shifting approximation

Most quantum dynamical and approximate approaches calculating thermal rate constants employ the J-shifting approximation[59] to obtain thermal rate constants for the full

TABLE II. Thermal rate constants k(T) in cm^3/s for the title reaction. Rigorous close-coupling results and J-shifting results on both the NN1 and SE PESs are given.

	NN1 PES		SE PES	
T (in K)	Close-coupling	J-shifting	Close-coupling	J-shifting
300	5.81×10^{-15}	6.85×10^{-15}	8.50×10^{-15}	1.86×10^{-14}
350	1.58×10^{-14}	1.77×10^{-14}	2.01×10^{-14}	3.86×10^{-14}
400	3.43×10^{-14}	3.81×10^{-14}	4.01×10^{-14}	7.22×10^{-14}
450	6.38×10^{-14}	7.20×10^{-14}	7.07×10^{-14}	1.23×10^{-13}
500	1.07×10^{-13}	1.23×10^{-13}	1.14×10^{-13}	1.93×10^{-13}
550	1.65×10^{-13}	1.93×10^{-13}	1.71×10^{-13}	2.84×10^{-13}
600	2.39×10^{-13}	2.85×10^{-13}	2.43×10^{-13}	3.98×10^{-13}
700	4.36×10^{-13}	5.40×10^{-13}	4.33×10^{-13}	6.95×10^{-13}

system from calculations ignoring the overall angular momentum ($J = 0$). It was shown previously that for the semi-empirical SE PES this is not a good approximation leading to errors up to 50%.[13,32] In Fig. 2, accurate results for the high-level NN1 PES including overall rotation are compared to quantum dynamical results obtained through J-shifting. Additionally, the same set of results is shown for the semi-empirical SE PES. For the SE PES, big differences of up to 50% between the close-coupling and J-shifting results are found, in accordance with the previous results.[13,32] For the NN1 PES, a different picture emerges as the overall J-shifting error is small. Errors due to J-shifting amount to 15% or less in the range of 300 K–600 K. At higher temperatures, a slightly larger deviation is found. However, this is not an effect due to the J-shifting but due to better convergence of the J-shifting results for the higher temperatures considered. Employing a higher reference temperature in the close-coupling results as presented in the supplementary material results in differences below 10% for the close-coupling and J-shifting results on the NN1 PES at higher temperatures. As was pointed out in previous work, the fit of the SE PES to the *ab initio* data is not great, in particular, around the transition state,[13,83] which results, e.g., in a large difference for the moments of inertia at the transition state when computed on the PES and with the *ab initio* calculations. As the moments of inertia are crucial for the J-shifting approximation, it is not surprising that J-shifting is not good for this PES. However, the NN1 PES was fitted with much more accuracy than the SE PES and reproduces the transition state region very well. Thus, it can be concluded that for the title reaction the overall rotational motion can be well separated and that J-shifting is reasonable. This validates the use of the J-shifting approximation in earlier approximate calculations on the NN1 PES.

C. Spin-orbit coupling

An additional source of error when comparing accurate calculations to experimental results or when employing calculated rate constants in kinetic models is the treatment of spin-orbit coupling. As most potential energy surfaces do not include spin-orbit coupling, an additional term has to be

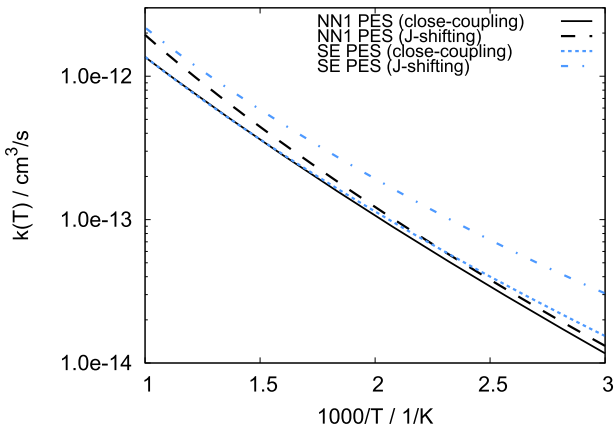

FIG. 2. Thermal rate constants k(T) in cm^3/s for the title reaction. Rigorous close-coupling results and J-shifting results on both the NN1 and SE PESs are given.

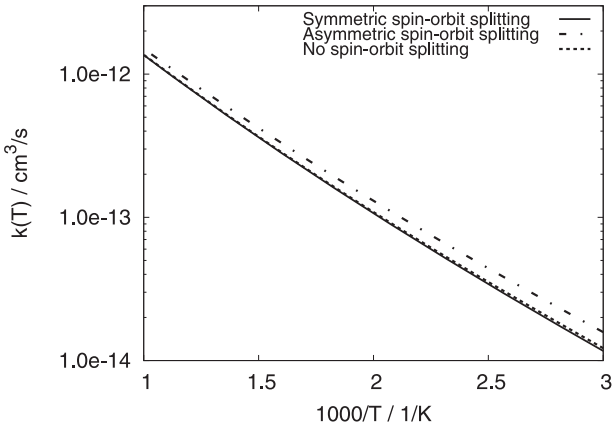

FIG. 3. Thermal rate constants k(T) in cm^3/s for the title reaction. Rigorous close-coupling results are given employing different treatments of the spin-orbit coupling. See the text for details.

included in the partition function. As given in Eqs. (10) and (11), there are two ways to do this. The first approach assumes that the given spin-orbit free state is the correct ground state and assumes that the spin-orbit excited state is ΔE_{elec} higher. The second approach assumes that the given spin-orbit free state is an equal average of both spin-orbit split states and thus that the true ground state is $\Delta E_{\text{elec}}/2$ lower and the spin-orbit excited state is $\Delta E_{\text{elec}}/2$ higher than the given state. The latter approach performs better for the $Cl + H_2 \rightarrow HCl + H$ reaction, where potentials with spin-orbit coupling and without spin-orbit coupling are available.[72] As both the SE and NN1 PESs are constructed from electronic structure data that do not include spin-orbit splitting, the latter approach is also the logical consistent way to account for spin-orbit splitting in this work. Please note, however, that several previous and also some recent work do use the former approach. Alternatively, the spin-orbit coupling can be neglected and a factor of two is employed in the partition function as only one of the initial electronic states is reactive.

Figure 3 presents results that ignore spin-orbit coupling and that include the spin-orbit coupling in the partition function, as described in Eqs. (10) and (11). Ignoring spin-orbit coupling matches the second strategy well, while results obtained from the symmetric and asymmetric splitting differ by up to 40% in the temperature range considered. Following Ref. 72 and the logical argument presented above, we assume that the second strategy is more accurate and all results presented in this work are obtained employing Eq. (11). It should be noted that the difference between the different ways to incorporate spin-orbit splitting is about the magnitude of the difference between the results presented here and the RPMD results,[58] which employ the first strategy.

V. CONCLUSION

Accurate thermal rate constants including overall rotation and employing a high-level *ab initio* potential energy surface are presented for the $H_2 + OH \rightarrow H_2O + H$ reaction. The rate constants agree very well with experimentally obtained rate constants. It is found that the J-shifting approximation is reasonable for the title reaction. This is in contrast to results

obtained on the semi-empirical SE PES.[13,32] Additionally, the importance of including spin-orbit coupling is highlighted. Differences in the treatment of the spin-orbit splitting can give errors in the rate constants of up to 40% at room temperature. As the title reaction is of atmospheric and astrochemical importance, accurate rate constants at low and ultra-low temperatures are of great interest. Highly accurate benchmark results as presented in this work are necessary to benchmark more approximate methods.

SUPPLEMENTARY MATERIAL

See supplementary material for basis set sizes and convergence tests.

ACKNOWLEDGMENTS

The author thanks Johannes Kästner and Uwe Manthe for helpful discussions.

[1] A. Wagner and M. Graff, Astrophys. J. **317**, 423 (1987).
[2] Y. Oba, N. Watanabe, T. Hama, K. Kuwahata, H. Hidaka, and A. Kouchi, Astrophys. J. **749**, 67 (2012).
[3] H. Cuppen and E. Herbst, Astrophys. J. **668**, 294 (2007).
[4] T. Lamberts, H. Cuppen, G. Fedoseev, S. Ioppolo, K.-J. Chuang, and H. Linnartz, Astron. Astrophys. **570**, A57 (2014).
[5] R. Atkinson, D. Baulch, R. Cox, R. Hampson, J. Kerr, and J. Troe, Atmos. Environ., Part A **26**, 1187 (1992).
[6] T. Rahn, J. M. Eiler, K. A. Boering, P. O. Wennberg, M. C. McCarthy, S. Tyler, S. Schauffler, S. Donnelly, and E. Atlas, Nature **424**, 918 (2003).
[7] S. Gligorovski, R. Strekowski, S. Barbati, and D. Vione, Chem. Rev. **115**, 13051 (2015).
[8] D. H. Zhang, M. A. Collins, and S.-Y. Lee, Science **290**, 961 (2000).
[9] C. Xiao, X. Xu, S. Liu, T. Wang, W. Dong, T. Yang, Z. Sun, D. Dai, X. Xu, D. H. Zhang *et al.*, Science **333**, 440 (2011).
[10] I. W. Smith and F. F. Crim, Phys. Chem. Chem. Phys. **4**, 3543 (2002).
[11] S. C. Althorpe and D. C. Clary, Annu. Rev. Phys. Chem. **54**, 493 (2003).
[12] M. Brouard, I. Burak, S. Marinakis, D. Minayev, P. O'Keeffe, C. Vallance, F. Aoiz, L. Banares, J. Castillo, D. H. Zhang *et al.*, Phys. Rev. Lett. **90**, 093201 (2003).
[13] U. Manthe and F. Matzkies, J. Chem. Phys. **113**, 5725 (2000).
[14] G. C. Schatz and H. Elgersma, Chem. Phys. Lett. **21**, 73 (1980).
[15] B. J. Braams and J. M. Bowman, Int. Rev. Phys. Chem. **28**, 577 (2009).
[16] B. Jiang, J. Li, and H. Guo, Int. Rev. Phys. Chem. **35**, 479 (2016).
[17] M. A. Collins, Theor. Chem. Acc. **108**, 313 (2002).
[18] M. Yang, D. H. Zhang, M. A. Collins, and S.-Y. Lee, J. Chem. Phys. **115**, 174 (2001).
[19] B. Fu, E. Kamarchik, and J. M. Bowman, J. Chem. Phys. **133**, 164306 (2010).
[20] J. Chen, X. Xu, X. Xu, and D. H. Zhang, J. Chem. Phys. **138**, 154301 (2013).
[21] E. M. Goldfield and S. K. Gray, J. Chem. Phys. **117**, 1604 (2002).
[22] T. Wu, H.-J. Werner, and U. Manthe, Science **306**, 2227 (2004).
[23] R. Welsch and U. Manthe, J. Chem. Phys. **137**, 244106 (2012).
[24] R. Welsch and U. Manthe, J. Chem. Phys. **138**, 164118 (2013).
[25] R. Welsch and U. Manthe, J. Chem. Phys. **142**, 064309 (2015).
[26] Y. Wang, Y. Li, and D. Wang, Sci. Rep. **7**, 40314 (2017).
[27] J. Li, J. Chen, D. H. Zhang, and H. Guo, J. Chem. Phys. **140**, 044327 (2014).
[28] W. H. Miller, J. Chem. Phys. **61**, 1823 (1974).
[29] W. H. Miller, S. D. Schwartz, and J. W. Tromp, J. Chem. Phys. **79**, 4889 (1983).
[30] D. H. Zhang and J. C. Light, J. Chem. Phys. **104**, 6184 (1996).
[31] F. Matzkies and U. Manthe, J. Chem. Phys. **106**, 2646 (1997).
[32] F. Matzkies and U. Manthe, J. Chem. Phys. **108**, 4828 (1998).
[33] U. Manthe, J. Chem. Phys. **128**, 064108 (2008).
[34] F. Huarte-Larrañaga and U. Manthe, Z. Phys. Chem. **221**, 171 (2007).
[35] U. Manthe, Mol. Phys. **109**, 1415 (2011).
[36] H.-D. Meyer, U. Manthe, and L. S. Cederbaum, Chem. Phys. Lett. **165**, 73 (1990).
[37] U. Manthe, H.-D. Meyer, and L. S. Cederbaum, J. Chem. Phys. **97**, 3199 (1992).
[38] R. Welsch, F. Huarte-Larranaga, and U. Manthe, J. Chem. Phys. **136**, 064117 (2012).
[39] R. Welsch and U. Manthe, Mol. Phys. **110**, 703 (2012).
[40] U. Manthe and R. Welsch, J. Chem. Phys. **140**, 244113 (2014).
[41] B. Zhao, Z. Sun, and H. Guo, J. Chem. Phys. **140**, 234110 (2014).
[42] R. Welsch and U. Manthe, J. Chem. Phys. **141**, 051102 (2014).
[43] R. Welsch and U. Manthe, J. Chem. Phys. **141**, 174313 (2014).
[44] R. Welsch and U. Manthe, J. Phys. Chem. Lett. **6**, 338 (2015).
[45] B. Fu, X. Shan, D. H. Zhang, and D. C. Clary, Chem. Soc. Rev. **46**, 7625 (2017).
[46] R. Ellerbrock and U. Manthe, Chem. Phys. **482**, 106 (2017).
[47] R. Ellerbrock and U. Manthe, J. Chem. Phys. **147**, 241104 (2017).
[48] H. Wang and M. Thoss, J. Chem. Phys. **119**, 1289 (2003).
[49] U. Manthe, J. Chem. Phys. **128**, 164116 (2008).
[50] U. Manthe, J. Chem. Phys. **105**, 6989 (1996).
[51] U. Manthe, J. Chem. Phys. **130**, 054109 (2009).
[52] F. Gatti, B. Lasorne, H.-D. Meyer, and A. Nauts, *Applications of Quantum Dynamics in Chemistry* (Springer, 2017).
[53] J. Kaestner, Wiley Interdiscip. Rev.: Comput. Mol. Sci. **4**, 158 (2014).
[54] S. Habershon, D. E. Manolopoulos, T. E. Markland, and T. F. Miller, Annu. Rev. Phys. Chem. **64**, 387 (2013).
[55] Y. V. Suleimanov, F. J. Aoiz, and H. Guo, J. Phys. Chem. A **120**, 8488 (2016).
[56] J. L. Bao and D. G. Truhlar, Chem. Soc. Rev. **46**, 7548 (2017).
[57] J. Meisner and J. Kästner, J. Chem. Phys. **144**, 174303 (2016).
[58] J. Castillo and Y. Suleimanov, Phys. Chem. Chem. Phys. **19**, 29170 (2017).
[59] J. M. Bowman, J. Phys. Chem. **95**, 4960 (1991).
[60] F. Matzkies and U. Manthe, J. Chem. Phys. **112**, 130 (2000).
[61] T. Yamamoto, J. Chem. Phys. **33**, 281 (1960).
[62] U. Manthe and W. H. Miller, J. Chem. Phys. **99**, 3411 (1993).
[63] U. Manthe, J. Chem. Phys. **102**, 9205 (1995).
[64] W. H. Thompson and W. H. Miller, J. Chem. Phys. **102**, 7409 (1995).
[65] U. Manthe and F. Matzkies, Chem. Phys. Lett. **252**, 71 (1996).
[66] D. H. Zhang and J. C. Light, J. Chem. Phys. **106**, 551 (1997).
[67] H. Wang, W. H. Thompson, and W. H. Miller, J. Chem. Phys. **107**, 7194 (1997).
[68] U. Manthe and F. Matzkies, Chem. Phys. Lett. **282**, 442 (1998).
[69] F. Matzkies and U. Manthe, J. Chem. Phys. **110**, 88 (1999).
[70] U. Manthe and R. Ellerbrock, J. Chem. Phys. **144**, 204119 (2016).
[71] T. J. Park and J. Light, J. Chem. Phys. **88**, 4897 (1988).
[72] U. Manthe, W. Bian, and W. Werner, Chem. Phys. Lett. **313**, 647 (1999).
[73] T. Wu, H.-J. Werner, and U. Manthe, J. Chem. Phys. **124**, 164307 (2006).
[74] F. Huarte-Larrañaga and U. Manthe, J. Chem. Phys. **117**, 4635 (2002).
[75] U. Manthe and F. Huarte-Larrañaga, Chem. Phys. Lett. **349**, 321 (2001).
[76] F. Huarte-Larrañaga and U. Manthe, J. Chem. Phys. **123**, 204114 (2005).
[77] M. H. Beck and H.-D. Meyer, Z. Phys. D: At., Mol. Clusters **42**, 113 (1997).
[78] U. Manthe, Chem. Phys. **329**, 168 (2006).
[79] A. Ravishankara, J. Nicovich, R. Thompson, and F. Tully, J. Phys. Chem. **85**, 2498 (1981).
[80] R. K. Talukdar, T. Gierczak, L. Goldfarb, Y. Rudich, B. M. Rao, and A. Ravishankara, J. Phys. Chem. **100**, 3037 (1996).
[81] R. Oldenborg, G. Loge, D. Harradine, and K. Winn, J. Phys. Chem. **96**, 8426 (1992).
[82] V. L. Orkin, S. N. Kozlov, G. A. Poskrebyshev, and M. J. Kurylo, J. Phys. Chem. A **110**, 6978 (2006).
[83] U. Manthe, T. Seideman, and W. H. Miller, J. Chem. Phys. **99**, 10078 (1993).